Electronic Structures of Peroxonickel(II) Bis(isocyanide) Complexes

Ian Bytheway and Michael B. Hall*

Department of Chemistry, Texas A&M University, College Station, Texas 77843

Received July 1, 1994[⊗]

Several electronic states of the peroxonickel(II) bis(isocyanide) molecule $Ni(O_2)(CNH)_2$ have been calculated using various *ab initio* methods in order to determine the ground state and the order of the low-lying excited states. Multireference configuration interaction calculations using natural orbitals predict a $^1A_1$ ground state, in agreement with the observed diamagnetism for the analogous *tert*-butyl-substituted molecule. The first excited state was found to be the $^3B_1$ state, formed by excitation of an electron from a dioxygen π_g orbital, whose nodal plane corresponds to the $Ni(O_2)(CNH)_2$ molecular plane, to the virtual nickel 3d orbital which lies in the NiO_2 plane. Natural orbital occupancies obtained from the multireference configuration interaction calculations show the $^1A_1$ state to be formally $Ni(II)-O_2^{2-}$, although substantial occupation of the formally unoccupied nickel 3d orbital suggests that the contribution to the molecular wave function from the superoxo-like $Ni(I)-O_2^-$ description is strong. The superoxo description dominates the lowest excited state ($^3B_1$), but here the singly occupied O_2 orbital is perpendicular to the NiO_2 plane. In addition to these two states, three other low-lying triplet states were calculated, and the charge densities (ϱ and $\nabla^2\varrho$) of all five states were examined.

Introduction

An interesting feature of the chemistry of dioxygen is its ability to bind to metal atoms in either an end- or side-on fashion. Understanding the origin of this behavior is important, not only from a general chemical perspective, *i.e.*, understanding why these different coordination modes exist, but also in a wider and perhaps more pragmatic sense as dioxygen complexation is important to both natural and synthetic chemical systems.

A variety of metal–dioxygen complexes have been studied using *ab initio* methods,[1] although, because of their biological importance, the majority of complexes studied are those containing iron or copper. Calculations have played an important part in understanding the nature of the iron–dioxygen bond and provided support for the end-on mode of dioxygen bonding to iron in the heme molecule.[1] Another important role of *ab initio* calculations was in establishing the correct ground state in the heme system, and large calculations, which account for the effects of electron correlation, have confirmed that the ground state for heme molecules is a closed-shell singlet and not a triplet state.[2] Oxygen carriers in anthropods utilize copper rather than iron, and calculations of model copper–dioxygen complexes have provided a means of comparing the effects of the possible modes of dioxygen bonding to known empirical data[3] from which the actual mode of dioxygen bonding may not be derived explicitly. From the viewpoint of synthetic chemistry, the coordination of dioxygen to other transition metals is equally important,[4] as in many cases these complexes act as catalysts for novel reactions.[5]

Dioxygen complexes of the late transition metals are homogeneous oxidation catalysts; for example, platinum–dioxygen complexes catalyze the oxidation of ketones to carboxylic acids,[6] while palladium–dioxygen complexes oxidize alkenes to epoxides.[7] Analogous catalytic reactions for nickel have not been developed,[8] though a few nickel complexes are known.[9] The only nickel–dioxygen complex which has been fully characterized is the peroxonickel(II) bis(*tert*-butyl isocyanide) complex **1**, which is diamagnetic[10] and has a square planar geometry,[11] as expected for a d^8 nickel complex.[12] INDO calculations[13] of **1** predicted the tetrahedral geometry to be higher in energy than the observed square planar geometry by 16 kcal mol^{-1}. No calculation of the energies separating the low-lying states was made at this level. Recently, a triplet ground state ($^3B_2$) for **2**, in which an isocyanide π^* orbital was singly occupied, was predicted to be more stable than the closed-shell singlet state.[14] The open-shell ground state obtained from these restricted Hartree–Fock calculations was used to explain the free radical pathway for the oxidation of organic compounds by (η^2-peroxo)-nickel(II) complexes. Because of the disagreement between these calculated results and experimentally observed diamag-

[⊗] Abstract published in *Advance ACS Abstracts,* June 15, 1995.

(1) For a review of theoretical studies of metal–dioxygen systems see: Bytheway, I.; Hall, M. B. *Chem. Rev.* **1994**, *94*, 639.
(2) (a) Yamamoto, S.; Kashiwagi, H. *Chem. Phys. Lett.* **1989**, *161*, 85. (b) Yamamoto, S.; Kashiwagi, H. *Chem. Phys. Lett.* **1993**, *205*, 306.
(3) Solomon, E. I.; Tuczek, F.; Root, D. E.; Brown, C. A. *Chem. Rev.* **1994**, *94*, 827.
(4) Brindley, P. B. In *The Chemistry of Peroxides*; Patai, S., Ed.; Wiley–Interscience: New York, 1983; p 807.
(5) Mimoun, H. In *The Chemistry of Peroxides*; Patai, S., Ed.; Wiley–Interscience: New York, 1983; p 463.
(6) Roundhill, D. M. In *Comprehensive Coordination Chemistry*; Wilkinson, G., Gillard, R. D.; McCleverty, J. A., Eds.; Pergamon Press: Oxford, 1987; Vol. 5, p 463.
(7) Maitlis, P. M.; Espinet, P.; Russell, M. J. H. *Comprehensive Organometallic Chemistry*; Wilkinson, G., Stone, F. G. A., Abel, E. W., Eds.; Pergamon Press: Oxford, 1982; p 258.
(8) (a) Jolly, P. W.; Wilke, G. *The Organic Chemistry of Nickel*; Academic Press: New York, 1974; Vol. 1, p 317. (b) Jolly, P. W. *Comprehensive Organometallic Chemistry*; Wilkinson, G., Stone, F. G. A., Eds.; Pergamon Press: New York, 1982; Vol. 6, p 132.
(9) Sacconi, L.; Mani, F.; Bencini, A. In *Comprehensive Coordination Chemistry*; Wilkinson, G., Gillard, R. D., McCleverty, J. A., Eds.; Pergamon Press: Oxford, 1987; Vol. 5, p 28.
(10) Otsuka, S.; Nakamura, A.; Tatsuno, Y. *J. Am. Chem. Soc.* **1969**, *91*, 6994.
(11) Matsumoto, M.; Nakatsu, K. *Acta Crystallogr.* **1975**, *B31*, 2711.
(12) Cotton, F. A.; Wilkinson, G. *Advanced Inorganic Chemistry* 5th ed.; Wiley-Interscience: New York, 1988; p 747.
(13) Tatsumi, K.; Fueno, T.; Nakamura, A.; Otsuka, S. *Bull. Chem. Soc. Jpn.* **1976**, *49*, 2164.
(14) Jørgensen, K. A.; Swanstrøm, P. *Acta Chem. Scand.* **1992**, *46*, 82.

0020-1669/95/1334-3741$09.00/0

netism, we present here new calculations for the ground state and various low-lying states of the peroxonickel bis(isocyanide) complex **3**.

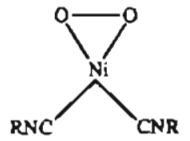

1 R = *tert*-butyl
2 R = CH_3
3 R = H

Theoretical Details

Calculations were performed on the peroxonickel(II) bis(isocyanide) molecule **3** with the experimental bond lengths and angles from the X-ray crystal structure of **1** and with the imposition of C_{2v} symmetry.[6] In addition, the *tert*-butyl substituents attached to the nitrogen atoms of the isocyanide ligands in the observed structure **1** were replaced by hydrogen atoms. This change should have little effect on the electronic structure of the nickel−dioxygen moiety, while reducing the amount of computation required. Calculations were performed using standard 3-21G double-ζ valence basis sets[15] for hydrogen, carbon, nitrogen, and oxygen, while for nickel a basis set of triple-ζ quality was constructed from the Huzinaga $3d^94s^1$ (4333/43/5) basis set.[16] This nickel basis set was split, and an extra p function (with a coefficient of one-third that of the preceding p function) was added to give a basis set with the overall contraction scheme of (43321/4211/311). All *ab initio* calculations were performed at Texas A&M University using the GAMESS-UK[17] software on a Silicon Graphics Indigo-R4000 workstation. Total charge densities were analyzed using the AIMPAC[18] and MOPLOT[19] software packages.

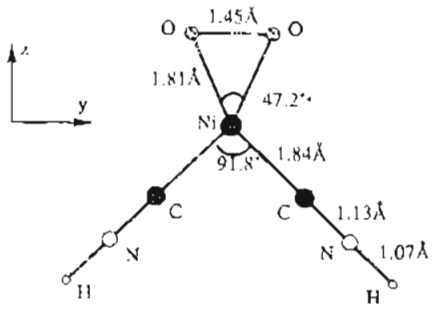

3

Results and Discussion

Definition and Characterization of States. A range of calculations for a singlet and four triplet electronic states of **3** (labeled in the C_{2v} coordinate system) were considered. Each state was obtained initially by occupying the molecular orbitals (MOs) in Figure 1 differently. The $^1A_1$ state was formed by doubly occupying each of the lowest nine orbitals in Figure 1, *i.e.*,

$$a_1(3\sigma_g)^2b_1(\pi_u{}^a)^2a_1(\pi_u{}^s)^2a_2(d_{xy})^2a_1(d_{z^2-y^2})^2b_1(d_{xz})^2b_2(d_{yz}+\pi_g{}^s)^2a_1(d_{x^2})^2a_2(\pi_g{}^a)^2$$

Four triplet states of different symmetry were then formed by exciting one electron from different doubly occupied orbitals into the low-lying $d_{yz}-\pi_g{}^s$ orbital, *i.e.*,

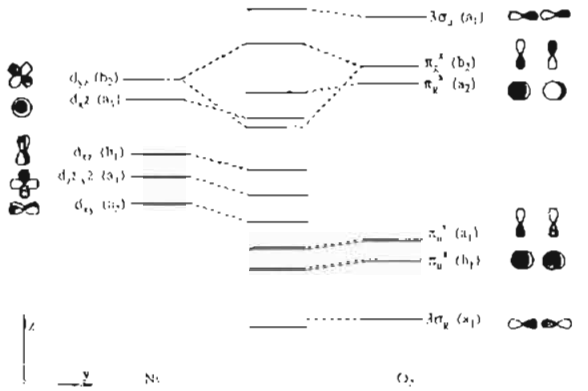

Figure 1. Molecular orbital diagram for the interaction between Ni and O_2 in **3**. The lower energy MOs belonging to the isocyanide ligand are not shown, although these were included in the active space during the CI calculations. The superscripts s and a denote whether or not the O_2 orbitals are symmetric or antisymmetric with respect to the NiO_2 plane. The ordering of the MOs is based on the results of the NO−CI(2ref) calculations, for example, the d_{xz} orbital is shown below the d_{x^2} orbital, since excitation of an electron from the d_{xz} orbital into the $d_{yz}-\pi_g{}^s$ orbital gave a state ($^3B_2$) with higher energy than the state ($^3A_2$) formed by excitation of an electron from the d_{x^2} orbital into the $d_{yz}-\pi_g{}^s$ orbital.

$^3B_1$	$a_2(\pi_g{}^a)^1b_2(d_{yz}-\pi_g{}^s)^1$
$^1B_2$	$a_1(d_{x^2})^1b_2(d_{yz}-\pi_g{}^s)^1$
$^3A_1$	$b_2(d_{yz}+\pi_g{}^s)^1b_2(d_{yz}-\pi_g{}^s)^1$
$^3A_2$	$b_1(d_{xz})^1b_2(d_{yz}-\pi_g{}^s)^1$

The energies for restricted Hartree−Fock (RHF) calculations of each of these states are given in Table 1, and the state separation energies are shown in Figure 2a. The important result obtained from these RHF calculations is that the lowest energy triplet state is the $^3B_1$ state, which is higher in energy than the $^1A_1$ state by 2.22 kcal mol^{-1} (see Figure 2a). In addition, this $^3B_1$ state is not the same as that described previously.[13] Comparison of singlet and triplet state energies obtained from RHF calculations do not, however, give the true relative energies separating open- and closed-shell states. Comparison of the energies of these states requires that electron correlation be included in the calculation of their energies.

In a RHF calculation, the only electron correlation included is a consequence of satisfying the antisymmetry requirement of the Pauli principle, *i.e.*, that electrons of the same spin have a very low probability of occupying the same region of space. A consequence of this is that only electrons of the same spin are correlated in an RHF calculation, resulting in some electron correlation being included in a triplet state calculation which is not in the singlet state. In order to treat all states equally, the remaining effects of electron correlation must be considered, which was done in this work using the method of configuration interaction (CI). In all of the CI calculations described here, the core space consisted of the Ni ($1s^22s^22p^63s^23p^6$), O($1s^22s^2$), C($1s^2$), N($1s^22s^2$), and σ(N−H) orbitals, while the active space consisted of the remaining 30 electrons and 72 orbitals. This rather large active space was chosen to ensure that the separation of the active and core orbitals was made at the same place for each state and that the same orbitals were used in all of the CI calculations.

After the initial RHF calculation for each state, a CI calculation with single and double excitations from the RHF reference configuration was performed with the RHF orbitals, *i.e.*, the orbitals for each state given above were used in building

(15) Binkley, J. S.; Pople, J. A.; Hehre, W. J. *J. Am. Chem. Soc.* **1980**, *102*, 939.
(16) Huzinaga, S., Ed. *Gaussian Basis Sets for Molecular Calculations*; Elsevier: Amsterdam, 1983.
(17) Guest, M. F.; Sherwood, P. *GAMESS-UK*, Revision B.0, S.E.R.C., Daresbury Laboratory, 1992.
(18) Biegler-König, F. W.; Bader, R. F. W.; Tang, T.-H. *J. Comput. Chem.* **1982**, *3*, 317.
(19) Sherwood, P.; MacDougall, P. J. The interactive MOPLOT package for the display and analysis of molecular wave functions comprising MOPLOT (Lichtenburger, D.), PLOTDEN (Bader, R. F. W.; Kenworthy, D. J.; Beddall, P. M.; Runtz, G. R.; Anderson, S. G.), SCHUSS (Bader, R. F. W.; Runtz, G. R.; Anderson, S. G.; Biegler-König, F. W.) and EXTREM (Bader R. F. W.; Biegler-König, F. W.).

Table 1. Energies (in au) Calculated at the Different Levels of Theory for Five Different Electronic States of the $Ni(O_2)(CNH)_2$ Complex

	$^1A_1$	$^3B_1$	$^3B_2$	$^3A_1$	$^3A_2$
RHF	−1838.946764	−1838.943220	−1838.937422	−1838.899499	−1838.924320
RHF-CI(1ref)	−1839.523042	−1839.513660	−1839.461824	−1839.458325	−1839.453530
NO-CI(1ref)	−1839.529446	−1839.514653	−1839.467690	−1839.458034	−1839.459591
NO-CI(2ref)	−1839.552195	−1839.534072	−1839.480313	−1839.477826	−1839.472469

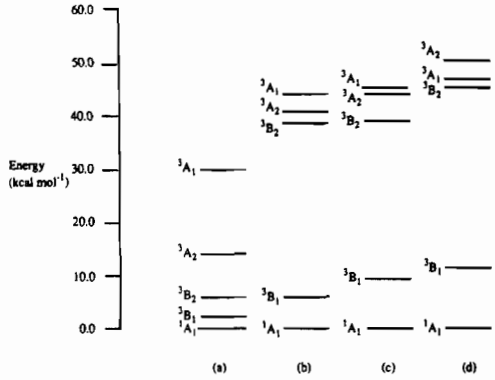

Figure 2. Energies in kcal mol^{-1} of the triplet states relative to the closed-shell $^1A_1$ state obtained at the various levels of theory: (a) RHF, (b) The RHF-CI(1ref), (c) NO-CI(1ref), and (d) NO-CI(2ref).

a configuration space where both one and two electrons were excited from the previously occupied orbital to the virtual ones. At this level of calculation, denoted RHF-CI in Table 1, the $^1A_1$ state is lower in energy than the $^3B_1$ state by 5.89 kcal mol^{-1} and significantly lower than the remaining $^3B_2$, $^3A_1$, and $^3A_2$ states (see Figure 2b). The lowering of the energy of the $^1A_1$ state with respect to the triplet states suggests that the singlet state is the correct description of the ground state, although a better description of the molecular wave functions for the different states will be needed for an accurate estimate of the energies separating them.

In order to improve the calculations for each of the five states being considered, the natural orbitals (NO) were obtained from each RHF-CI calculation and then used to perform a second CI calculation. The results of these calculations are denoted NO-CI(1ref) in Table 1. Natural orbitals are desirable because CI calculations employing them converge faster than those which use SCF orbitals and fewer configuration state functions are required to reach comparable levels of accuracy.[20] At this level of theory, the energy of the $^1A_1$ is lower than the lowest triplet state ($^3B_1$) by 9.28 kcal mol^{-1}, *i.e.*, a more accurate description of the states using natural orbitals increases the stability of the singlet state with respect to the triplet states (Figure 2c).

The final set of calculations was performed using these same natural orbitals in a multireference CI with two reference configurations—the RHF configuration and the second most important configuration obtained from the NO-CI(1ref) calculation. These results, denoted NO-CI(2ref) in Table 1, show that the $^1A_1$ state is now lower in energy than the $^3B_1$ state by 11.37 kcal mol^{-1} (Figure 2d). The second reference configuration is particularly important for the ground state because the excitations to the low-lying ($d_{yz}-\pi_g^s$) orbital make important contributions. Thus, as the accuracy of the method used to calculate the energy of each state is increased, so is the relative stability of the singlet state. We conclude from these results that the ground state of **3**, and also of the observed **1**, is $^1A_1$.

The two important configurations used in the NO-CI(2ref) calculations and their contributions to the overall description of each state are given in Table 2. For each state, the leading configuration corresponds to the RHF configuration and contributes approximately 80% to the wave function, with smaller contributions made by configurations obtained by the excitation into the $3\sigma_u$ and $d_{yz}-\pi_g^s$ orbitals. The lowering of the singlet state energy with respect to the triplet state energies is also reflected in the contribution to the overall wave function made by the leading configuration which is 79% for the $^1A_1$ state, compared to around 82% in each of the triplet states. In addition, the contribution of the next most important configuration for the $^1A_1$ wave function is also slightly more (4% in the singlet state compared to approximately 2% for each of the triplet states).

The natural orbitals involving the nickel 3d and dioxygen π_g orbitals of the $^1A_1$ state, calculated at the NO-CI(2ref) level of theory, are shown in Figure 3. The $3d_{xy}$ (Figure 3a), $3d_{xz}$ (Figure 3c), and $3d_{x^2}$ (Figure 3d) orbitals are all localized on the nickel atom, while the nickel $3d_{z^2-y^2}$ orbital (Figure 3b) and $3d_{yz}+\pi_g^s$ (Figure 3e) have ligand bonding character. Of these bonding orbitals, the $3d_{yz}+\pi_g^s$ combination shows the greatest amount of bonding character. The dioxygen antibonding π_g^a orbital (Figure 3f), plotted in the plane perpendicular to the NiO_2 plane which contains both oxygen atoms, is strongly localized on the O_2 part of the molecule. The last orbital shown is the $3d_{yz}-\pi_g^s$ (Figure 3g), which is clearly the antibonding combination of the nickel $3d_{yz}$ and dioxygen π_g^s orbitals. The natural orbitals for the triplet states are not shown, as these were found to be similar to those obtained for the $^1A_1$ state; thus, the triplet states can be thought of as having the same orbitals, with different occupation patterns, as the singlet state.

The occupancies of the natural orbitals (*i.e.*, obtained from the NO-CI(2ref) calculations) are given in Table 3 and reflect the importance of near-degenerate contributions to the description of the molecule made by the additional reference configurations. In particular, the rather large occupation of the $d_{yz}-\pi_g^s$ orbital in the $^1A_1$ state (0.13 electron) suggests that, although the $Ni^{II}-O^{2-}$ peroxo description is formally appropriate, there is a contribution from the superoxo $Ni^{I}-O^{-}$ description. Finally, it is also important to note that no low-lying states involving the single occupation of isocyanide antibonding orbitals were found.

Charge Density Analysis. For each of the calculations described in the previous section, the total charge density (ϱ) and its Laplacian ($\nabla^2\varrho$) were analyzed. Atomic charges, obtained by integrating over the basin of the atom,[21] were calculated for each of the atoms in **3** at both the RHF and NO-CI(2ref) levels of theory and are given in Table 4. For each particular type of calculation (*i.e.*, across a row), the charges reflect the electronic differences between each state, while a comparison of the charges for each atom obtained at the different levels of theory (*i.e.*, the RHF result versus the NO-CI(2ref) result) shows how electron correlation alters the total charge density distribution of a state.

At the RHF level, the calculated charge for Ni in the $^1A_1$ state is 1.087 and for the $^3B_1$ state is 0.780. This difference in charge can be attributed to the formal transfer of an electron from the doubly occupied and predominantly dioxygen π_g^a orbital to the $d_{yz}-\pi_g^s$ Ni orbital. This results in an increase in

(20) Löwdin, P.-O. *Phys. Rev.* **1955**, *97*, 1474.

(21) Bader, R. F. W. *Atoms in Molecules: A Quantum Theory*; Oxford University Press: Oxford, 1990.

Table 2. Two Reference Configurations Used in the NO-CI(2ref) Calculations for Each State of **1** Considered

state	important configurations[a]	%[b]
$^1A_1$	$(3\sigma_g)^2(\pi_u^a)^2(\pi_u^s)^2(d_{xy})^2(d_{z^2-y^2})^2(d_{xz})^2(d_{yz}+\pi_g^s)^2(d_{x^2})^2(\pi_g^a)^2$	80
	$(d_{yz}+\pi_g^s)^2(d_{yz}-\pi_g^s)^0 \rightarrow (d_{yz}+\pi_g^s)^0(d_{yz}-\pi_g^s)^2$	4
$^3B_1$	$(3\sigma_g)^2(\pi_u^a)^2(\pi_u^s)^2(d_{xy})^2(d_{z^2-y^2})^2(d_{xz})^2(d_{x^2})^2(d_{yz}+\pi_g^s)^2(\pi_g^a)^1(d_{yz}-\pi_g^s)^1$	85
	$(3\sigma_g)^2(3\sigma_u)^0 \rightarrow (3\sigma_g)^1(3\sigma_u)^1$ and $(\pi_u^a)^2(\pi_g^a)^1 \rightarrow (\pi_u^a)^1(\pi_g^a)^2$	2
$^3B_2$	$(3\sigma_g)^2(\pi_u^a)^2(\pi_u^s)^2(d_{xy})^2(d_{z^2-y^2})^2(d_{xz})^2(d_{yz}+\pi_g^s)^2(d_{x^2})^1(\pi_g^a)^2(d_{yz}-\pi_g^s)^1$	81
	$(3\sigma_g)^2(3\sigma_u)^0 \rightarrow (3\sigma_g)^0(3\sigma_u)^2$	2
$^3A_1$	$(3\sigma_g)^2(\pi_u^a)^2(\pi_u^s)^2(d_{xy})^2(d_{z^2-y^2})^2(d_{xz})^2(d_{yz}+\pi_g^s)^1(d_{x^2})^2(\pi_g^a)^2(d_{yz}-\pi_g^s)^1$	85
	$(3\sigma_g)^2(3\sigma_u)^0 \rightarrow (3\sigma_g)^1(3\sigma_u)^1$ and $(\pi_u^a)^2(\pi_g^a)^1 \rightarrow (\pi_u^a)^1(\pi_g^a)^2$	2
$^3A_2$	$(3\sigma_g)^2(\pi_u^a)^2(\pi_u^s)^2(d_{xy})^2(d_{z^2-y^2})^2(d_{xz})^1(d_{yz}+\pi_g^s)^2(d_{x^2})^2(\pi_g^a)^2(d_{yz}-\pi_g^s)^1$	84
	$(3\sigma_g)^2(3\sigma_u)^0 \rightarrow (3\sigma_g)^0(3\sigma_u)^2$	2

[a] Only the main reference configuration is written out in full, using the orbitals shown in Figure 1. For the other configuration, only those orbitals which have different occupancies relative to the main are shown. [b] The square of the CI coefficient.

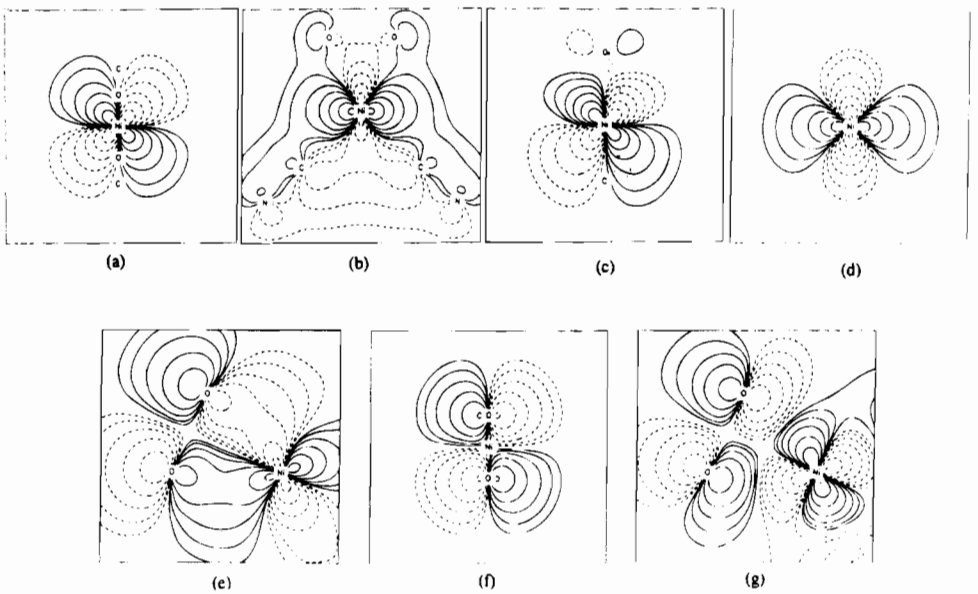

Figure 3. Plots of the natural orbitals shown qualitatively in Figure 1, obtained from the NO-CI(2ref) calculation of the $^1A_1$ state: (a) Ni $3d_{xy}$, (b) Ni $3d_{z^2-y^2}$, (c) Ni $3d_{xz}$, (d) Ni $3d_{x^2}$, (e) $3d_{yz}+\pi_g^s$, (f) O_2 π_g^a, and (g) $d_{yz}-\pi_g^s$. These orbitals are essentially the same as those in the various triplet states which were formed by excitation of an electron from the doubly occupied orbitals of the $^1A_1$ state (a–f) into the $d_{yz}-\pi_g^s$ orbital (g).

Table 3. Natural Orbital Occupancies Obtained from the NO-CI(2ref) Calculations of **1**

	natural orbital occupancies[a]										
state	$3\sigma_g$	π_u^a	π_u^s	d_{xy}	$d_{z^2-y^2}$	d_{xz}	$d_{yz}+\pi_g^s$	d_{x^2}	π_g^a	$d_{yz}-\pi_g^s$	$3\sigma_u$
$^1A_1$	1.97	1.99	1.98	1.98	1.98	1.98	1.88	1.98	1.99	0.13	0.03
$^3B_1$	1.94	1.95	1.99	1.98	1.98	1.98	1.99	1.98	1.04	1.00	0.06
$^3B_2$	1.94	1.99	1.98	1.99	1.98	1.99	1.97	1.00	1.99	1.02	0.06
$^3A_1$	1.92	1.99	1.95	1.98	1.98	1.98	1.03	1.98	1.99	1.01	0.07
$^3A_2$	1.94	1.99	1.98	1.98	1.98	1.00	1.97	1.99	1.99	1.01	0.06

[a] Natural orbital occupancies of the orbitals shown in Figure 1. The natural orbital occupation numbers for the lower energy orbitals included in the CI are not shown. These orbitals have occupancies close to 2.0.

Table 4. Atomic Charges for the Atoms in **1**, Calculated Using the RHF and NO-CI(2ref)) Charge Densities

atom	calc type	$^1A_1$	$^3B_1$	$^3B_2$	$^3A_1$	$^3A_2$
Ni	RHF	1.087	0.780	1.346	0.786	1.320
	NO-CI(2ref)	0.893	0.785	1.196	0.812	1.156
O	RHF	−0.649	−0.417	−0.758	−0.425	−0.754
	NO-CI(2ref)	−0.521	−0.393	−0.662	−0.418	−0.654
C	RHF	1.007	0.989	0.976	0.987	0.975
	NO-CI(2ref)	0.918	0.887	0.887	0.887	0.888
N	RHF	−1.462	−1.503	−1.453	−1.499	−1.445
	NO-CI(2ref)	−1.401	−1.424	−1.380	−1.417	−1.372
H	RHF	0.561	0.544	0.562	0.544	0.563
	NO-CI(2ref)	0.558	0.540	0.558	0.541	0.559

the Ni population for the $^3B_1$ state, *i.e.*, lower positive charge. At the NO-CI(2ref) level, this difference is less pronounced because of the importance of the $d_{yz}-\pi_g^s$ MO to the description of the $^1A_1$ state. Likewise, the charge on Ni in the $^3A_1$ state also reflects the fact that this state was obtained by the transfer of an electron from the predominantly dioxygen $d_{yz}+\pi_g^s$ orbital to the predominantly nickel $d_{yz}-\pi_g^s$ orbital. As before, this difference in charge with respect to the $^1A_1$ state is not as marked at the NO-CI(2ref) level. The $^3B_2$ and $^3A_2$ states show the largest positive charge on Ni at the RHF level, which is also significantly lessened at the NO-CI(2ref) level. The Ni charges in these states are more positive than in the other states, as they involve the transfer of a nearly pure nickel d electron into the $d_{yz}-\pi_g^s$ orbital. In these states, the $d_{yz}-\pi_g^s$ orbital does not have predominantly Ni character but is indeed a mixture of Ni (d_{yz}) and O_2 (π_g^s) orbitals. Thus, for these states, there is significant transfer of charge into the antibonding π_g^s dioxygen orbital, resulting in increased negative charge on the dioxygen ligand. The charges on the carbon, nitrogen, and hydrogen atoms are similar for all states at both levels of theory.

The value of ϱ at the bond critical points (*i.e.*, the point of

Table 5. Values of ϱ (in e Å^{-3}) at Various Bond Critical Points in **1**, Obtained from the RHF and NO-CI(2ref) Calculations

bond	calculation	$^1A_1$	$^3B_1$	$^3B_2$	$^3A_1$	$^3A_2$
ϱ(Ni−O))	RHF	0.127	0.114	0.125	0.107	0.125
	NO-CI(2ref)	0.124	0.117	0.125	0.107	0.127
ϱ(Ni−C)	RHF	0.116	0.115	0.116	0.115	0.120
	NO-CI(2ref)	0.117	0.118	0.118	0.117	0.122
ϱ(O−O)	RHF	0.242	0.242	0.241	0.242	0.241
	NO-CI(2ref)	0.238	0.237	0.236	0.236	0.236

minimum charge density along the path of maximum charge density joining two atoms[21]) in the various states of **1**, and at the different levels of calculation, can also be compared. It is interesting to note that, in general, there is very little difference in the value of ϱ at the bond critical point for the same state, calculated at different levels of theory (see Table 5), although there is some difference between the states. The value of ϱ at the bond critical point may be related to bond strength,[20] and from the values in Table 5, it appears that, relative to the $^1A_1$ state, the Ni−O bond is weakened in the $^3B_1$ and $^3A_1$ states, while it is unaffected in both the $^3B_2$ and $^3A_2$ states. A quantitative estimate of the differences in bond strength is not possible from these data, but they do suggest that the first two excited states of **1** may be more amenable to Ni−O bond cleavage. The values of ϱ at the bond critical point for the O−O and Ni−C bonds are roughly the same in all of the states and at both levels of calculation (the high degree of consistency is due in part to the identical geometry used for all these states).

The Laplacian of the charge density ($\nabla^2\varrho$), which reveals where charge is locally concentrated or depleted, was examined for the various states—although no significant differences in $\nabla^2\varrho$ are expected as a consequence of using different levels of theory (other than small changes in sizes or positions of maxima[22]). Plots of $\nabla^2\varrho$ for the $^1A_1$ and $^3B_1$ states, calculated using the NO-CI(2ref) wave functions, are shown in Figures 4a and 4b, respectively.

The collection of different types of critical points in $\nabla^2\varrho$ at a characteristic distance (for example, corresponding to the distance between the nucleus and valence electrons) from an atom is termed its atomic graph.[21] The atomic graph is analogous to the molecular graph, the difference being that the molecular graph describes how atoms are bonded within a molecule, while the atomic graph is particular to each atom in the molecule and describes how charge is distributed in each atom. The atomic graph for Ni in the $^1A_1$ state has four charge concentration maxima situated in the plane of the molecule between the Ni−O and Ni−C bonds. Thus, the core density of the metal atom is not spherical and is distorted, similar to that found in previous calculations of molecules containing metal atoms.[23] The atomic graph of nickel in the $^3B_1$ state of **1** is the same, although the distortion of the nickel core is less pronounced. An explanation for this is that the $^3B_1$ state is formed by singly occupying the $d_{yz}-\pi_g^s$ orbital, which is nearly a pure d_{yz} orbital in this state, and addition of this orbital to the description of the nickel core density results in a more spherical charge density distribution. The atomic graph of the $^3A_1$ state is also similar and also has less pronounced distortions of the core charge density.

The $^3B_2$ and $^3A_2$ states were formed by excitation of electrons from lower-lying nickel orbitals, and this resulted in the formation of atomic graphs for the nickel atom different from

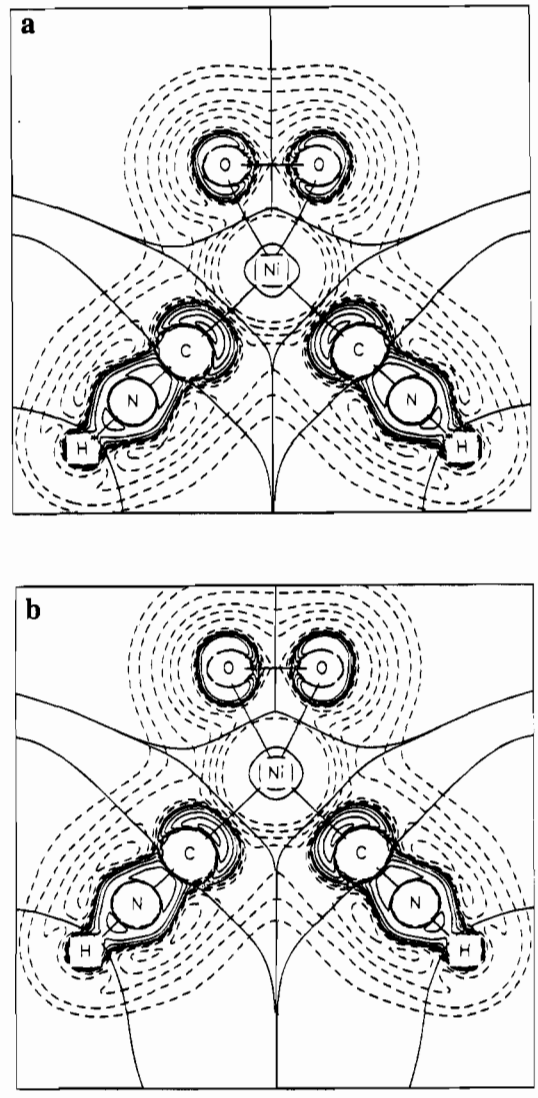

Figure 4. Plots of the Laplacian of the charge density ($\nabla^2\varrho$) for **1** with the atomic boundaries overlaid. Full contours denote regions of charge concentration ($\nabla^2\varrho < 0$) and dashed contours denote regions of charge depletion ($\nabla^2\varrho > 0$)): (a) $^1A_1$ state and (b) $^3B_1$ state.

those described above. There are eight charge concentration maxima in the nickel core in the $^3B_2$ state, arranged in a cube. This atomic graph is derived from that of nickel in the $^1A_1$ state by the splitting of each of the four maxima in the $^1A_1$ state into two. The atomic graph for the $^3A_2$ state consists of six maxima, arranged in an octahedron which has two vertices in the plane of the molecule (one maximum between the nickel−oxygen bond and one between the nickel−carbon bond) and four in the plane perpendicular to the molecule. In the $^3A_2$ state, the d_{xz} orbital is singly occupied, so charge is more concentrated in the *xy* plane (which gives the "equatorial" plane of the octahedral atomic graph) as well as in the plane of the molecule because of the doubly occupied d_{x^2} orbital (which contributes the "axial" plane of the octahedral atomic graph).

The atomic graph for the oxygen atom changes on going from the ground state to the first excited state, consistent with the transfer of an electron from the π_g^a orbital into the $d_{yz}-\pi_g^s$ orbital. In the $^1A_1$ state, the π_g^a orbital is doubly occupied, and for each oxygen atom, two charge concentrations are located above and below the plane of the molecule. In the $^3B_1$ state, the two charge concentration maxima belonging to oxygen are located in the molecular plane, as in this state the π_g^s orbital is nearly doubly occupied while the π_g^a orbital is singly occupied. For each of the remaining triplet states, the atomic graphs are

(22) Gatti, C.; MacDougall, P. J.; Bader, R. F. W. *J. Chem. Phys.* **1988**, *88*, 3792.
(23) (a) MacDougall, P. J.; Hall, M. B.; Bader, R. F. W.; Cheeseman, J. R. *Can. J. Chem.* **1989**, *67*, 1842. (b) Bytheway, I.; Gillespie, R. J.; Bader, R. F. W. To be submitted.

essentially the same as that in the ground state, as in each case the occupation of orbitals involving dioxygen, and hence its total density, is unchanged.

Conclusion

Ab initio calculations of the peroxonickel(II) bis(isocyanide) complex **1** which included electron correlation predict that the ground state of this molecule is a closed-shell singlet state, in agreement with the experimental results[9] for the analogous *tert*-butyl-substituted molecule **2**. The first excited state is a $^3B_1$ state, which is 11.37 kcal mol^{-1} higher in energy than the singlet ground state at the NO-CI(2ref) level of theory. The other triplet states are more than 40 kcal mol^{-1} above the ground state at this same level of theory (see Figure 2). Experimental studies of the oxidation of organic molecules by nickel peroxide complexes suggested that these reactions occur via a free-radical pathway,[24] and for this reason, the $^3B_2$ state obtained from previous calculations[14] was postulated as a viable ground state. Although our results suggest that the ground states for these complexes are closed-shell singlets, the low-lying $^3B_1$ (not $^3B_2$) state may participate in such reactions.

Wave functions were obtained from the experimental geometry with different levels of theory and for different electronic states, and the differences in charge density with respect to both the change in method of calculation and the change in electronic structure were examined. At the different levels of theory, atomic charges at the correlated level of theory reflect the partial occupation of (formally) virtual orbitals, while there is little difference in the topology of either ϱ or $\nabla^2\varrho$. Between states, the calculated atomic charges and the topologies of ϱ and $\nabla^2\varrho$ reflect the differences in the orbital occupancies which define the various states.

These calculations are instructive, as they demonstrte quite clearly the need for electron correlation when comparing open- and closed-shell states. The energy separating the singlet ground state and the lowest energy triplet state is large enough that basis set improvement will not alter the relative order of these two states, although such improvement should provide a better quantitative estimate of the energy separation.

Acknowledgment. Support from the National Science Foundation, Grants CHE 91-13634 and 94-23271, and the Robert A. Welch Foundation, Grant No. A-648, is gratefully acknowledged. We also thank Z. Lin and M. A. Pietsch for helpful discussions during the course of this work.

IC940773M

(24) Terabe, S.; Nakata, T. *J. Chem. Soc., Perkin Trans. II* **1972**, 2163.